ORIGINAL CONTRIBUTION

Rhinology, 48, 300-304, 2010

Topography of the rabbit paranasal sinuses as a prerequisite to model human sinusitis*

Christophe Casteleyn[1*], Pieter Cornillie[1], Astrid Hermens[1], Denis Van Loo[2], Luc Van Hoorebeke[2], Wim Van den Broeck[1], Paul Simoens[1]

[1] Department of Morphology, Faculty of Veterinary Medicine, Ghent University, Ghent, Belgium
[2] Centre for X-Ray Tomography, Ghent University, Ghent, Belgium

SUMMARY

Background: *Anatomical studies of the rabbit paranasal cavities are impelled by the increasing interest in the rabbit model to investigate human sinusitis. Although several such studies have already been performed, the topography of the rabbit dorsal conchal and maxillary sinuses is described ambiguously and the existence of the ethmoidal, frontal and sphenoidal sinuses is controversial.*

Methodology: *The paranasal cavities were investigated using corrosion casting, gross and histological cross-sectioning, and micro-CT scanning of rabbit noses followed by computerized three-dimensional reconstruction.*

Results: *Micro-CT scanning was most useful to illustrate the dorsal conchal sinus, the large maxillary sinus consisting of a dorsal and a ventral recess, and the sphenoidal sinus. All these sinuses are paired and symmetrical. A large connection is present between the dorsal conchal sinus and the maxillary sinus resulting in one large conchomaxillary cavity. The sphenoidal sinus lies most caudal and is surrounded by the presphenoid bone. The openings from the nasal cavity into the conchomaxillary cavity and the sphenoidal sinus are very small.*

Conclusions: *The absence of frontal and ethmoidal sinuses in any of the rabbits examined is a major difference between the rabbit and human sinuses. The rabbit maxillary sinus seems most appropriate for experimental work.*

Key words: rabbit, paranasal sinuses, nasal cavity, micro-CT, three-dimensional reconstruction

INTRODUCTION

Interest in animal models to facilitate the study of human sinus disease is currently increasing. The rabbit is often promoted as the experimental animal of choice since the relative volume of the nasal cavity in this species resembles that of humans [1,2]. The rabbit model has already proven its utility in the fine-tuning of therapeutic procedures to treat sinusitis or other sinus-related pathologies. Such procedures include, amongst others, maxillary floor augmentation allowing the insertion of dental implants of sufficient length [3,4], and sinus obliteration, which is often necessary in various conditions such as recalcitrant disease or large mucoeceles [5].

Despite the common use of the rabbit model, the paranasal sinuses of this animal species have only seldom been studied anatomically. Data about the presence of the dorsal conchal and maxillary sinuses in the rabbit are consistent, but their descriptions and nomenclature are somewhat ambiguous [6-9]. The presence of the ethmoidal sinus in the rabbit has been demonstrated by Kerschner et al. [10], although Kelemen [7] does not report such a sinus but ethmoidal cells instead. Kelemen [7], Barone [11] and Hartcourt-Brown [9] clearly report the absence of the frontal sinus in the rabbit. In contrast, Prince [12] describes the presence of small frontal sinuses, while Altman et al. [5] and Peltola et al. [13] describe experiments in which they obliterated these sinuses. The sphenoidal sinus, which is surrounded by the presphenoid bone, has been described controversially as a very reduced [7,11] or a large [6,12] sinus in the rabbit.

From this short literature review, it might be clear that many characteristics of the rabbit paranasal cavities remain obscure. The confusing nomenclature used by different authors has contributed to the lack of consistency between the various reports concerning the anatomy of the rabbit sinuses. Therefore, this paper aims to visualize the rabbit sinuses with a state-of-the-art technique. A detailed anatomical description of the rabbit sinuses, using the official anatomical nomenclature [14,15], could allow a more accurate translation of experimental results from rabbit models to humans.

*Received for publication: November 24, 2009; accepted: December 9, 2009

DOI:10.4193/Rhin09.193

MATERIALS AND METHODS

Animals

A total number of 20 adult New Zealand White rabbits of both gender, weighing approximately 2 kg, were used. The animals were euthanised for educational reasons by injecting 1 ml T61® (Embutramide 200 mg, Mebenzoniumiodide 50 mg, Tetracaine hydrochloride 5 mg, Dimethylformamide et aqua dest. q.s. ad 1 ml, Intervet, Mechelen, Belgium) in the lateral ear vein. After death, the bodies were decapitated in the atlanto-occipital joints and the heads were immediately stored at 4°C (5 specimens) or -20°C (15 specimens).

Corrosion casting (Figure 1A)

Five ml of Batson's #17® corrosion casting solution (Brunschwig Chemie, Amsterdam, The Netherlands) was gently injected into the nasal cavities of three rabbit heads via the nostrils, after clamping off the trachea. After injection, the heads were placed in cold water for 30 min and subsequently macerated in 25% potassium hydroxide (Roth, Karlsruhe, Germany) for 2 days. The macerated heads were rinsed with water and dried under a vented hood. The remaining specimens, which comprised the skull and the polymerized injected casting solution, were evaluated and photographed with a stereomicroscope (Olympus SZX7, Olympus Belgium, Aartselaar, Belgium).

Gross freeze-sectioning (Figure 1B)

Using a band saw, the noses of 13 frozen rabbit heads were cut transversely into 5 mm thick slabs, and two frozen heads were cut longitudinally in rostrocaudal direction along the median plane. Both longitudinally sectioned heads and three cross-sectioned noses were examined after a short defrosting time using the stereomicroscope (Olympus SZX7, Olympus Belgium) linked to a digital camera (Olympus ColorView, Olympus Belgium). The 5 mm thick slabs of the three cross-sectioned noses were further dissected to reveal additional anatomical information. The cross-sections from the remaining ten heads were defrosted and fixed in 3.5% neutral buffered formaldehyde at room temperature for further histological processing.

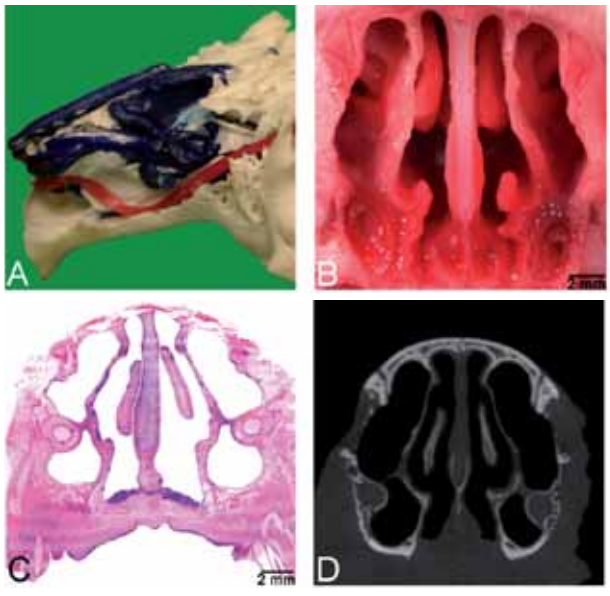

Figure 1. Representative images obtained by the various techniques that were used to examine the anatomy of the rabbit paranasal cavities: (A) Injection of the paranasal cavities (blue) and the lacrimal duct (red) with Batson's #17® casting solution, (B) cutting 5 mm thick slabs from frozen heads using a band saw, (C) histological sectioning of the rabbit nose at intervals of 0.5 mm after skull decalcification, and (D) micro-CT scanning of the rabbit head.

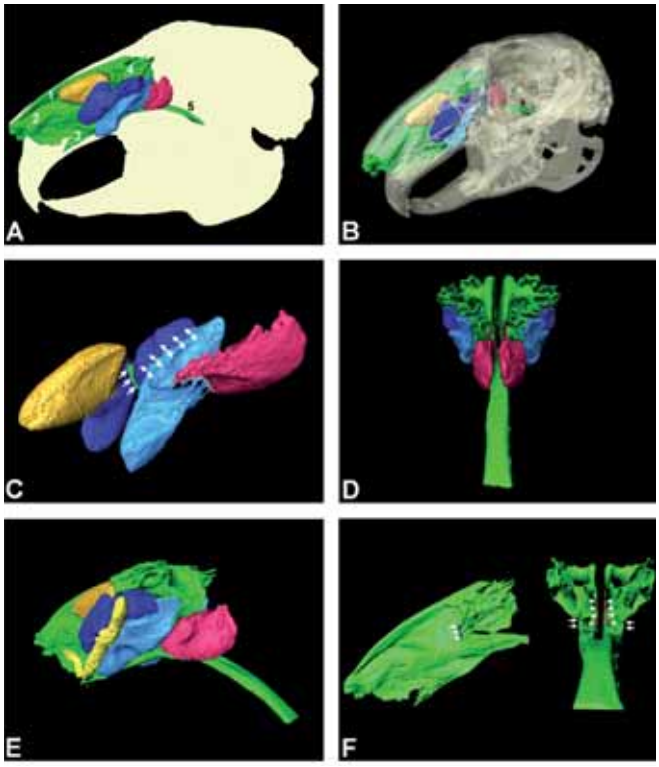

Figure 2. Three-dimensional reconstructions of the rabbit paranasal sinuses.
A: Left lateral view of the rabbit nasal cavity (green) consisting of the dorsal (1), middle (2) and ventral (3) nasal meatuses and the ethmoidal meatuses (4), the dorsal conchal sinus (ochre), the dorsal and ventral recesses of the maxillary sinus (dark and light blue, respectively) and the sphenoidal sinus (purple). The nasopharyngeal meatus (5) is the ventrocaudal continuation of the nasal cavity. B: Similar view showing the anatomical topography of the rabbit sinuses within the skull. C: Medial view of the right-sided rabbit sinuses showing the orifices of the conchomaxillary cavity and the sphenoidal sinus into the nasal cavity (white and black arrows, respectively). Notice the large caudal connection between the dorsal and ventral recesses of the maxillary sinus (curved double arrows). D: Caudal view of the rabbit nasal and paranasal cavities clearly demonstrating the air-filled spaces (green) in between the extensive ethmoidal labyrinth. E: Left caudolateral view of the rabbit nasal and paranasal cavities. The lacrimal canal (yellow) is located laterally and crosses the recesses of the maxillary sinus. F: Left lateral and caudal views of the air-filled spaces within the rabbit nasal cavity (green) showing its connections with the conchomaxillary cavity (arrows) and the sphenoidal sinuses (arrowheads).

Histological analysis (Figure 1C)

All fixed cross-sections from the noses of the ten rabbit heads were decalcified at room temperature by immersion in Stewart's solution consisting of 90 ml distilled water, 5 ml formic acid and 5 ml 3.5% buffered formaldehyde [16,17]. The cross-sections were subsequently dehydrated in a tissue processor (Microm STP420D, Prosan, Merelbeke, Belgium) and embedded in paraffin (Microm EC 350-1 embedding station, Prosan). From the paraffin blocks, 8 μm thick sections were cut at intervals of 0.5 mm (Microm HM 360 microtome, Prosan). All histological sections were mounted on slides and automatically stained with haematoxylin and eosin (Sakura Linear Stainer II, Sakura Finetek Europe B.V., Zoeterwoude, The Netherlands). A motorised light microscope (Olympus BX 61, Olympus Belgium) linked to a digital camera (Olympus DP 50, Olympus Belgium) was used for histological examination.

Micro-CT (Figure 1D)

One rabbit head and a rabbit skull, obtained by macerating the soft tissues in 42% sodium hypochlorite (VWR International NV/SA, Leuven, Belgium), were scanned using an in house developed micro-CT system consisting of a closed X-ray tube (Hamamatsu Photonics K.K., Tokyo, Japan) with directional target and an A-Si flat panel detector (Varian, Salt lake City, Utah, USA). The tube operated at 90 kV and 900 projection images were recorded in 30 minutes. The CT-data were reconstructed with a voxel pitch of 58 μm using Octopus® software [18], resulting in 1500 slices of 1000 x 1000 pixels. This large data set was entered in the Amira® 4.0 software (Visage Imaging GmbH, Berlin, Germany) for three-dimensional (3D) reconstruction.A specific volume of interest was defined by using the Lattice Access module and loaded in the computer's memory. After noise reduction by edge-preserved smoothening, image segmentation was performed by histogram thresholding, hereby partitioning the dataset into bone tissue, soft tissue and air-filled spaces. Different components of the latter voxel set were subsequently manually subdivided and attributed to the different sinuses and the nasal cavity by using the segmentation tools in the image segmentation editor. In a similar way, the lacrimal canals were extracted from the soft tissue. After resampling the data set to a voxel pitch of 232 μm, surface reconstruction was performed without additional smoothening.

RESULTS

The micro-CT analysis of the fresh rabbit head combined with 3D-reconstruction was most useful to illustrate the topography of the sinuses. All figures presented in this paper are therefore computerized 3D-reconstructions from that particular case. The examination of the rabbit skull using micro-CT was less informative since the soft tissues of the nose contribute largely to the formation of the rabbit paranasal sinuses. The other techniques were used to obtain additional information and to verify the data obtained by the micro-CT technique. The most important disadvantage of the corrosion casting technique was the presence of air bubbles in the casts, which made the results hard to interpret. The gross freeze-sectioning technique was very useful to gain 3D insight into the topography of the paranasal cavities and allowed further dissection of the noses, albeit within 5 mm thick slabs. Finally, the histological sections were not only examined to verify the exact locations of some structures of interest, but also rendered 3D insight, since subsequent sections were only separated by a small interval of 0.5 mm. The rabbit paranasal cavities are paired and comprise a dorsal conchal sinus, a large maxillary sinus that consists of a dorsal and a ventral recess, and a sphenoidal sinus (Figures 2A and B).

The oblong dorsal conchal sinus lies most dorsal in the rabbit nasal cavity, and is situated ventrolateral to the dorsal nasal meatus (Figure 2A). It is a pneumatized cavity within the dorsal nasal concha. Its rostral border is located caudodorsal to the ventral nasal concha which is only present in the rostral half of the nasal cavity. The caudal border is located just rostral to the ethmoturbinal bones, which line the ethmoidal meatuses. As a result, the dorsal conchal sinus is situated dorsally in the middle third part of the nasal cavity (Figures 2A and B).

The maxillary sinus is the largest paranasal cavity, being composed of two recesses. It is present in the region of the cribrous zone of the maxilla and extends towards the rostral orbital edge (Figure 2B). The oblong dorsal recess is located lateral to the middle nasal meatus and directly ventral to the dorsal conchal sinus (Figure 2A). Both paranasal cavities are connected to each other by a very large opening, which is situated in the rostral half of the dorsal recess of the maxillary sinus (Figures 2A and C). The ventral recess of the maxillary sinus, which has a similar ovoid shape as the dorsal recess, lies ventral to the latter and more towards the median plane (Figure 2D). Its ventral side shows impressions caused by the sockets of the upper premolars (Figures 2A, B and E). The rostral halves of both recesses are crossed by the lacrimal canal (Figure 2E), while their caudal halves are largely connected to each other (Figure 2C). The rostral edges of both recesses are located at the same level as the rostral pole of the dorsal conchal sinus. In contrast, the maxillary sinus extends more caudally and it is twice as long as the dorsal conchal sinus (Figure 2E). As a result, the caudal half of the maxillary sinus is located ventral to the ethmoidal meatuses. The ventral recess of the maxillary sinus extends more caudally than its dorsal counterpart (Figures 2A and E). As such, it covers the rostral part of the sphenoidal sinus (Figures 2A, B and E). The large conchomaxillary cavity formed by the dorsal conchal sinus and both recesses of the maxillary sinus only have a small, slit-like common opening into the nasal cavity (Figures 2C and F).

The sphenoidal sinus is located most caudally and medially and is surrounded by the presphenoid bone (Figures 2A, B and E). It has a more or less discoidal shape and is connected with the middle nasal meatus through a small slit-like rostral opening (Figures 2C and F).

No frontal or ethmoidal sinuses were observed in any of the rabbits investigated in the present study. The endoturbinal bones are well developed in the rabbit and delineate an air-filled ethmoidal labyrinth (Figures 2A, E and F). Like the frontal bones, however, the ethmoidal bones are not pneumatized.

DISCUSSION

The present study demonstrates that the rabbit paranasal cavities are paired and consist of the dorsal conchal sinus, the maxillary sinus, and the sphenoidal sinus. The data generated in our study concerning the topography of the dorsal nasal concha are in accordance with earlier observations. However, the nomenclature used previously is ambiguous and should be discussed briefly. The dorsal conchal sinus, which was named the *nasal marsupium* by Bensley [6] and Kelemen [7], has its origin in the pneumatization of the dorsal nasal concha. The nature of this dorsal nasal concha is also controversial, as most authors agree that it is partly formed by the first of the four endoturbinal bones [19,20], whereas Kelemen [7] states that it is located within a different nasoturbinal bone.

According to literature data and our results, the maxillary sinus is located lateral to the nasal cavity and ventral to the dorsal conchal sinus [6,7,9,11]. Its lateral wall lies adjacent to the cribrous zone of the maxillary bone [6]. Barone [11] and Hartcourt-Brown [9] mention that the maxillary sinus consists of a single straight cavity. However, our results support the description by Kelemen [7] that this sinus comprises a dorsal and a ventral recess, which communicate through a wide opening, and that the maxillary sinus opens with a very large orifice in the dorsal nasal concha. The resulting large conchomaxillary cavity is connected with the nasal cavity by a narrow slit-like orifice. This refutes the assertion of Hartcourt-Brown [9] that two separate openings into the nasal cavity are present at the rostral ends of the dorsal conchal sinus and the maxillary sinus, respectively. The presence of a single and small connection between the nasal cavity and the large conchomaxillary cavity makes the latter vulnerable to pathologies [7].

The sphenoidal sinus, which is surrounded by the presphenoid bone, is considered by Kelemen [7] and Barone [11] as being very reduced in the rabbit. The present study and the reports of Bensley [6] and Prince [12] do, however, demonstrate the opposite.

An ethmoidal sinus has been demonstrated in the rabbit by Kerschner et al. [10]. In contrast, Kelemen [7] does not describe an ethmoidal sinus, but *ethmoidal cells* instead; the latter are represented by the open spaces between the ethmoturbinals, while the ethmoturbinals themselves are not pneumatized. However, the term *ethmoidal cells* is inaccurate since it can only be applied to define the cavities within the ethmoturbinal bones [11]. *Ethmoidal cells* are present in humans [11,21], while the open space between the ethmoturbinal bones in the rabbit represents the middle nasal meatus [14].

Some controversy about the existence of the rabbit frontal sinus is present in literature. Prince [12] mentioned that the frontal sinuses are small in the rabbit since their frontal bones are not well developed. In contrast, Kelemen [7], Barone [11] and Hartcourt-Brown [9] reported the absence of the frontal sinus in this species. According to Barone [8], the dorsal conchal sinus is sometimes described as the frontal sinus. The latter nomenclature has been used by Altman et al. [5] when reporting their obliteration experiments of the rabbit sinuses. The presence of a frontal sinus has also been mentioned in the work of Peltola et al. [13] who describe the diploic marrow cavity within the frontal bones as the frontal sinus.

The micro-CT technique is very useful to examine the rabbit paranasal cavities. In contrast to the scanning itself, the manual labeling of the various sinuses and the final 3D-reconstruction using the software Amira® is very labour intensive. Moreover, the interpretation of the native CT-images (Figure 1D), which is a prerequisite for a correct 3D-reconstruction, requires some experience. In our study, the histological and the gross free-sectioning techniques were therefore valuable. These techniques also pointed out that the 3D-reconstruction of the fresh rabbit head that was scanned in the micro-CT is representative for all 20 adult New Zealand White rabbits we examined.

It can be concluded that rabbits possess a dorsal conchal sinus, a maxillary sinus and a sphenoidal sinus, but no ethmoidal and frontal sinuses. The absence of the latter two sinuses is a major difference between rabbits and humans [21]. The assumption that the rabbit maxillary sinus is most appropriate for experimental work could therefore be confirmed.

ACKNOWLEDGEMENTS

The authors would like to thank L. Standaert and P. Vervaet for their excellent technical assistance.

AUTHORSHIP CONTRIBUTION

C. Casteleyn, P. Cornillie and A. Hermens conducted the study, performed the experiments and interpreted the obtained results. D. Van Loo and L. Van Hoorebeke performed the micro-CT scanning. W. Van den Broeck and P. Simoens critically reviewed the manuscript.

CONFLICT OF INTEREST

None declared

REFERENCES

1. Gizurarson S. Animal models for intranasal drug delivery studies: a review article. Acta Pharm Nord. 1990; 2: 105-122.
2. Illum L. Nasal delivery. The use of animal models to predict performance in man. J Drug Target. 1996; 3: 427-442.
3. Watanabe K, Niimi A, Ueda M. Autogenous bone grafts in the rabbit maxillary sinus. Oral Surg Oral Med Oral Pathol. 1999; 88: 26-32.
4. Xu H, Shimizu Y, Ooya K. Histomorphometric study of the stability of newly formed bone after elevation of the floor of the maxillary sinus. Br J Oral Maxillofac Surg. 2005; 43: 493-499.

5. Altman JI, Eloy JA, Hoch BL, Munoz CM, Shohet MR. Demineralized bone matrix and fat autograft in a rabbit model of frontal sinus obliteration. Otolaryngol Head Neck Surg. 2007; 137: 264-268.
6. Bensley BA. Practical anatomy of the rabbit. 6th edition. Toronto: The University of Toronto, 1938.
7. Kelemen G. The nasal and paranasal cavities of the rabbit in experimental work. A M A Arch Otolaryngol. 1955; 61: 497-512.
8. Barone R. Splanchnologie I. In: Barone R, ed. Anatomie Compareé des Mammifères Domestiques, Tome 3. 3ième édition. Paris: Vigot éditeurs, 1997.
9. Hartcourt-Brown F. Textbook of rabbit medicine. London: Butterworth-Heinemann, 2002.
10. Kerschner JE, Cruz MJ, Beste DJ, Donahue KM, Kehl KSK. Computed tomography vs. magnetic resonance imaging of acute bacterial sinusitis: a rabbit model. Am J Otolaryngol. 2000; 21: 298-305.
11. Barone R. Ostéologie. In: Barone R, ed. Anatomie Compareé des Mammifères Domestiques, Tome 1. 4ième édition. Paris: Vigot éditeurs, 1999.
12. Prince JH. The Rabbit in Eye Research. Springfield: Thomas books, 1994.
13. Peltola MJ, Aitasola KM, Suonpää JTK, Yli-Urpo A, Laippala PJ. In vivo model for frontal sinus and calvarial bone defect obliteration with bioactive glass S53P4 and hydroxyapatite. J Biomed Mater Res 2001; 58: 261-269.
14. Habel RE. Splanchnologia. In: Schaller O, ed. Illustrated Veterinary Anatomical Nomenclature. Stuttgart: Ferdinand Enke Verlag, 1992; 140-233.
15. Anonymous. Nomina Anatomica Veterinaria, 5th edition, World Association of Veterinary Anatomists. Hamburg, Columbia, Ghent, Sapporo. Internet reference: http://www.wava-amav.org.
16. Gooding H, Stewart D. A comparative study of histological preparations of bone which have been treated with different combinations of fixatives and decalcifying fluids. Lab J. 1932; 7: 55.
17. Casteleyn C, Broos AMC, Simoens P, Van den Broeck W. Nasal cavity-associated lymphoid tissue (NALT) in the rabbit. Vet Immunol Immunopathol. 2010; 133: 212-218.
18. Dierick M, Masschaele B, Van Hoorebeke L. Octopus, a fast and user-friendly tomographic reconstruction package developed in LabView (R). Meas Sci Technol. 2004; 15: 1366-1370.
19. Popesko P, Rajtová V, Horák J. A Colour Atlas of the Anatomy of Small Laboratory Animals, Vol. 1: Rabbit and Guinea Pig. London: Wolfe Publishing Ltd, 1992.
20. Barone R, Pavaux C, Blin PC, Cuq P. Atlas d'Anatomie du Lapin – Atlas of Rabbit Anatomy. Paris: Masson & Compagnie, 1973.
21. Witmer L, Ridgely RC. The paranasal air sinuses of predatory and armored dinosaurs (Archosauria: Theropoda and Ankylosauria) and their contribution to cephalic structure. Anat Rec. 2008; 291: 1362-1388.

Dr. Christophe Casteleyn, DVM, MSc
Department of Morphology
Faculty of Veterinary Medicine
Ghent University
Salisburylaan 133
B-9820 Merelbeke
Belgium

Tel.: +32-9-264 7715
Fax: +32-9-264 7790
E-mail: Christophe.Casteleyn@ugent.be